We are IntechOpen, the world's leading publisher of Open Access books
Built by scientists, for scientists

1

Hardware-In-the Loop Simulation System Construction for Spacecraft On-orbit Docking Dynamics, Ideas, Procedural and Validation

Tongli Chang
School of Electrical and Mechanical Engineering, Northeast Forestry University,
School of Electrical and Mechanical Engineering, Harbin Institute of Technology,
P. R. China

1. Introduction

The Hardware-In-the-Loop (HIL) simulation system for on-orbit docking dynamics is a large-scale complex test equipment. It establishes working conditions for the docking mechanism similar with those on orbit. The kernel of above dynamics HIL simulation system is a mechanical force and movement actions simulator. Besides the mechanical force and movement actions simulator, it also includes an environmental simulator, a micro-gravity simulator and so on.

In a narrow mind, the HIL simulation system for on-orbit docking dynamics refers to the mechanical force and movement action simulator. It is a feedback system which consists of the dynamics simulation model and real-time simulaton computer, the hardwares under test, the force and torque sensor, the motion simulator. The research topic of this paper is limited in above narrow mind.

The HIL simulation system for on-orbit docking dynamics is a key technology that played important roles in the lunar excursion of America and in the assembling and re-supplying of Russian MIR space station. Morden space programme enhance the requirements to the HIL simulation for spacecraft docking dynamics. International Space Station (ISS) program also required that the ISS Common Berthing Mechanism (CBM) testing on ground simulator should be performed under operational vacuum and thermal conditions (Office of NRBMP, 1999).

In the early days, the physical simulators played main roles in docking dyniamics tests. Because of the development of computor and the complexity of modern docking mechanism, the HIL simulation technology is applied in the docking dynamics simulation. The dynamic docking test system (DDTS) is setup in US (Gates & Graves, 1974), and the integated testing system for docking mechanism was built in former Soviet (Peng et al., 1992). In1980s, docking dynamic test facility (DDTF) was created for testing the handles-latch docking mechanism (Crimbert & Marchal, 1987). National space development agency of Japan built the rendezvous and docking operation test system (RDOTS) testing three-points handles-latch docking mechanism (Lange & Martin, 2002).

The HIL simulation for spacecraft on-orbit docking is a attractive and promising research field. Lim et al. (1989) modeled and simulated the Stewart platform of DDTS. They pointed out the inertia matrix has tendency to decouple when the mass of the legs increasing, for purpose of increasing the rigidity, and relative to the platform. But the inertia power matrix does not show any noticeable general tendency. Ananthakrishnan et al. (1996) developed a prediction based feed forward filter to enhance the simulation of contact forces and rebound velocities during the space docking. They used the off-line acquisition and least-squares procedure to define the pre-filter. But the characteristic of the simulation/hardware interface with the pre-filter is not clearly discussed. Zhang (1999) presented the scheme of 6-DOF HIL simulation system for docking. Guan (2001) simulated the spacecraft docking dynamics with mathematic simulation and pointed out that rigid-body model of spacecraft could meet the demand of the research on docking dynamics. Kawabe et al. (2001) adopted a high speed zero gravity motion simulator, whose frequency response is higher than 40Hz, to setup a HIL simulation system to research the collision and impact dynamics under zero gravity. They also validated the HIL simulation system with a drop shaft test. Huang et al. (2005) presented the spacecraft docking simulation using HIL simulator with Stewart platform and spring-mass payload. Yan et al. (2007) established a Space docking hybrid simulation prototype experiment system and stabilized it through adding superfluity digital damp. The docking dynamics calculation method was setup with spacecrafts docking in space. Tian et al. (2007) simulated the movement simulator in integrate test platform for docking mechanism. Zhao et al. (2007) analyzed the dynamometry scheme for semi-physical simulation platform of space docking mechanism and simulated with single-sensor and double-sensor schemes separately. The mathematic motion model of two spacecrafts was set up with two-spacecraft docking model. Zhao & Zhang (2008) analyzed the stability of the whole system of space docking dynamics simulation with simplified HIL simulation system based on mass-spring-damp simulated object. Under the proportion controller condition, the stability of the HIL simulation is analyzed. Wu et al. (2008) took the electro-hydraulic Stewart of the HIL simulation for on-orbit docking dynamics as a research object, designed a fuzzy-immune PID control of a 6-DOF parallel platform for docking simulation.

This paper will summarize the research results of author in the HIL simulation for on-orbit docking dynamics, and present a novel HIL simulation system construction idea based on simulation/hardware interface. Then, the HIL simulation system building procedurals based on it are developed. At last, validations of them are done with experimental test.

Even though the HIL simulation system design procedural discussed in this paper is based on the spacecraft on-orbit docking dynamics, it can meet the demands of other applications.

2. Aim and task of HIL simulation for spacecraft on-orbit docking dynamics

The aim of the HIL simulation for spacecraft on-orbit docking dynamics is to re-emerge the dynamic process of two spacecrafts on-orbit docking on the earth surface.

The tasks of the HIL simulation for spacecraft on-orbit docking dynamics include testing docking mechanism, checking buffer characteristics, simulating the dynamic process of two spacecrafts docking on orbit, defining parameters of docking mechanism, re-emerging troubles of actual spacecraft docking to help finding solution, checking the initial docking conditions of spacecraft docking process, testing the action and counteraction of spacecraft docking process, and so on.

As a large-scale experimental equipment, the HIL simulation system for spacecraft on-orbit docking dynamics should meet the following requirements to complete its simulation task:

1. Ability to simulate the docking process of various spacecrafts.

2. Ability to check or test various docking mechanisms.
3. Ability to test the actual physical docking mechanism and evaluate its performance.
4. Possibility to output and record necessary process parameters of the experimental test.
5. Feasibility to permit human being participates in the simulation.

Then, four attributes of system design of HIL simulation for spacecraft on-orbit docking dynamics are brought forward, they are the stability of the dynamics feedback system, the accuracy of re-emerging the dynamic process, the robust ability of the delay compensator and the adaptability to the docking mechanism and to the spacecraft. In another words, they are four fundamental problems of system design of HIL simulation for spacecraft on-orbit docking dynamics (Chang et al., 2008).

3. Analysis on spacecraft on-orbit docking dynamics

3.1 Initial conditions of on-orbit docking

The initial capturing conditions of two on-orbit docking spacecrafts are shown below

Axial approaching velocity	+0.35 m/ sec ;
Radial approaching velocity	-0.10 ~ +0.10 m/ sec ;
Radial deflection	-0.30 ~ +0.30 m ;
Pitch and yaw deflection	-7.0 ~ +7.0º ;
Roll deflection	-15.0 ~ +15.0 º ;
Pose angle velocity	-1.0 ~ +1.0 º/ sec .

Since the dynamic process of the spacecraft on-orbit docking does always converge, the initial conditions of on-orbit docking are often the utmost working conditions of the HIL simulation system for spacecraft on-orbit docking dynamics. Usually, 6DOF's operational capabilities of the HIL simulation system (Office of NRBMP, 1999):

- Positional tolerance of ±1.27mm and ±0.10degrees.
- Motion range of ±5 degrees for roll, pitch, and yaw; ±0.15m for translation in the horizontal plane; and 0.61m for vertical travel.
- Payload weight of 1135kg.

3.2 Segmentation of simulated system

Since the hard wares under test in the HIL simulation system are docking mechanisms, then the spacecraft on-orbit docking system can be segmented into two parts, shown in Figure 1. The active docking mechanism on chaser vehicle and the passive docking mechanism on target vehicle is classified as the hardwares under test, which is simulated with physical model. And the rest of the simulated system which consists of two spacecraft bodies are described with the mathematical model, which is translated into a programme which runs on a real-time simulation computer.

3.3 Dynamics model of on-orbit docking spacecraft bodis

The reference frame $\mathbf{e}(OXYZ)$ is set on the ground, it is inertia reference frame. Chaser vehicle body frame $\mathbf{e}_1(O_1X_1Y_1Z_1)$ is set at the mass centre of the chaser vehicle, and target vehicle body frame $\mathbf{e}_2(O_2X_2Y_2Z_2)$ is set at the mass centre of the target vehicle. $\mathbf{e}_3(O_3X_3Y_3Z_3)$ and $\mathbf{e}_4(O_4X_4Y_4Z_4)$ are at the geometry centre of the assembling surface between docking mechanism and spacecraft body. The directions of the reference frames are shown in Figure 2. The position and pose of spacecraft is defined in Figure 3. Euler angles are defined in Figure 4.

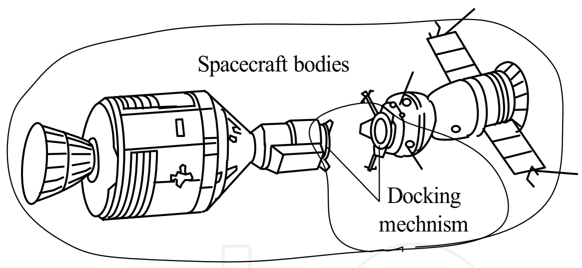

Fig. 1. Segmentation of simulated system

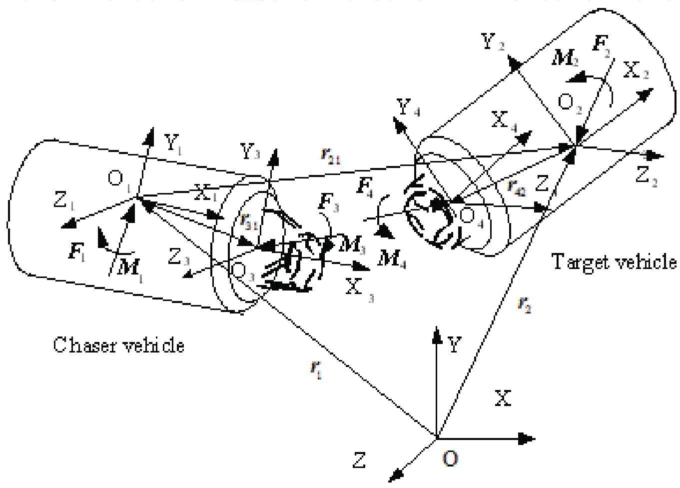

Fig. 2. On-orbit docking spacecraft bodies

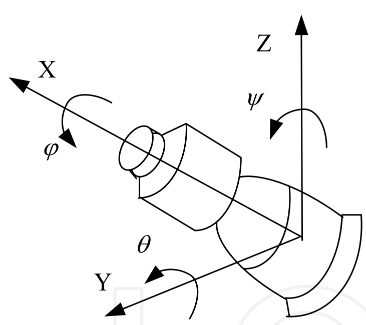

Fig. 3. Definition of position and pose

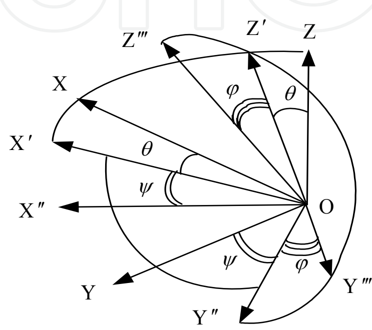

Fig. 4. Definition of Euler angle

When A stands for the transferring matrix from reference frame (OXYZ) to frame $(\mathrm{OX''Y'''Z'''})$, then

$$\mathbf{A}=\begin{bmatrix} \mathrm{c}\theta\cdot\mathrm{c}\psi & \mathrm{s}\varphi\cdot\mathrm{s}\theta-\mathrm{c}\varphi\cdot\mathrm{c}\theta\cdot\mathrm{s}\psi & \mathrm{c}\varphi\cdot\mathrm{s}\theta+\mathrm{s}\varphi\cdot\mathrm{c}\theta\cdot\mathrm{s}\psi \\ \mathrm{s}\psi & \mathrm{c}\varphi\cdot\mathrm{c}\psi & \text{-}\mathrm{s}\varphi\cdot\mathrm{c}\psi \\ -\mathrm{s}\theta\cdot\mathrm{c}\psi & \mathrm{s}\varphi\cdot\mathrm{c}\theta+\mathrm{c}\varphi\cdot\mathrm{s}\theta\cdot\mathrm{s}\psi & \mathrm{c}\varphi\cdot\mathrm{c}\theta-\mathrm{s}\varphi\cdot\mathrm{s}\theta\cdot\mathrm{s}\psi \end{bmatrix}. \tag{1}$$

Where $\mathrm{s}(\cdot)\overset{\Delta}{=}\sin(\cdot)$; $\mathrm{c}(\cdot)\overset{\Delta}{=}\cos(\cdot)$.

The roll, yaw and pitch angles of vehicle i can be work out with angle velocities of its pose.

$$\begin{pmatrix}\dot{\psi}_i\\ \dot{\theta}_i\\ \dot{\varphi}_i\end{pmatrix}=\begin{pmatrix}0 & \cos(\varphi_i)/\cos(\theta_i) & -\sin(\varphi_i)/\cos(\theta_i)\\ 0 & \sin(\varphi_i) & \cos(\varphi_i)\\ 1 & -\cos(\varphi_i)tg(\theta_i) & \sin(\varphi_i)tg(\theta_i)\end{pmatrix}\begin{pmatrix}\omega_{ix}\\ \omega_{iy}\\ \omega_{iz}\end{pmatrix}=\mathbf{N}\begin{pmatrix}\omega_{ix}\\ \omega_{iy}\\ \omega_{iz}\end{pmatrix}. \tag{2}$$

The force F_3 and torque M_3 come from active docking mechanism to the chaser vehicle are defined in $\mathbf{e}_3(\mathrm{O_3X_3Y_3Z_3})$, the other equivalent force F_1 and torque M_1 acting on chaser vehicle are defined in $\mathbf{e}_1(\mathrm{O_1X_1Y_1Z_1})$. The control signals to the chaser vehicle can be included in F_1 and M_1.

As well, the force F_4 and torque M_4 come from passive docking mechanism to the target vehicle are defined in $\mathbf{e}_4(\mathrm{O_4X_4Y_4Z_4})$, the other equivalent force F_2 and torque M_2 acting on chaser vehicle are defined in $\mathbf{e}_2(\mathrm{O_2X_2Y_2Z_2})$. The control signals to the target vehicle can be included in F_2 and M_2.

Through equation derivation (Chang et al., 2007e), the docking dynamics model of spacecraft body is gained, it can be describe with Figure 5.

$\mathbf{R}_1$ stands for the direction cosine matrix of frame $\mathbf{e}_1(\mathrm{O_1X_1Y_1Z_1})$ to frame $\mathbf{e}(\mathrm{OXYZ})$, $\mathbf{R}_2$ is the direction cosine matrix of frame $\mathbf{e}_2(\mathrm{O_2X_2Y_2Z_2})$ to frame $\mathbf{e}(\mathrm{OXYZ})$, $\mathbf{R}_{21}$ is the direction cosine matrix of frame $\mathbf{e}_2(\mathrm{O_2X_2Y_2Z_2})$ to frame $\mathbf{e}_1(\mathrm{O_1X_1Y_1Z_1})$. And some symbols are defined as:

$$\overset{\circ}{(\ )}\overset{\Delta}{=}\frac{{}^{\mathrm{b}}\mathrm{d}}{\mathrm{d}t}(\ ),\ \overset{\bullet}{(\ )}\overset{\Delta}{=}\frac{{}^{\mathrm{r}}\mathrm{d}}{\mathrm{d}t}(\ ),\ \overset{\circ\circ}{(\ )}\overset{\Delta}{=}\frac{{}^{\mathrm{b}}\mathrm{d}^2}{\mathrm{d}t^2}(\ ),\ \overset{\bullet\bullet}{(\ )}\overset{\Delta}{=}\frac{{}^{\mathrm{r}}\mathrm{d}^2}{\mathrm{d}t^2}(\ ).$$

3.4 Dynamic charateristics of docking mechanism

The docking mechanism is an important constituent of the HIL simulation system and of the simulated object system. The dynamic characteristic of docking mechanism plays important roles in the dynamic characteristic of the spacecraft on-orbit docking.

For an example, the APAS 89 docking mechanism is an inner guided petal androgynous peripheral assembly system, whose mechanical structure is Stewart platform. But the motions of six actuators of the Stewart platform are differential and not stand-alone (Kang, 1999). So the rigidity and damp characteristics of APAS 89 is very complicate.

Yu et al.(2004) set up the model of the APAS 89 docking mechanism with Adams software, which is a dynamics simulation and analysis software tool kit. Dynamics characteristics of the docking mechanism can be tested with its Adams model.

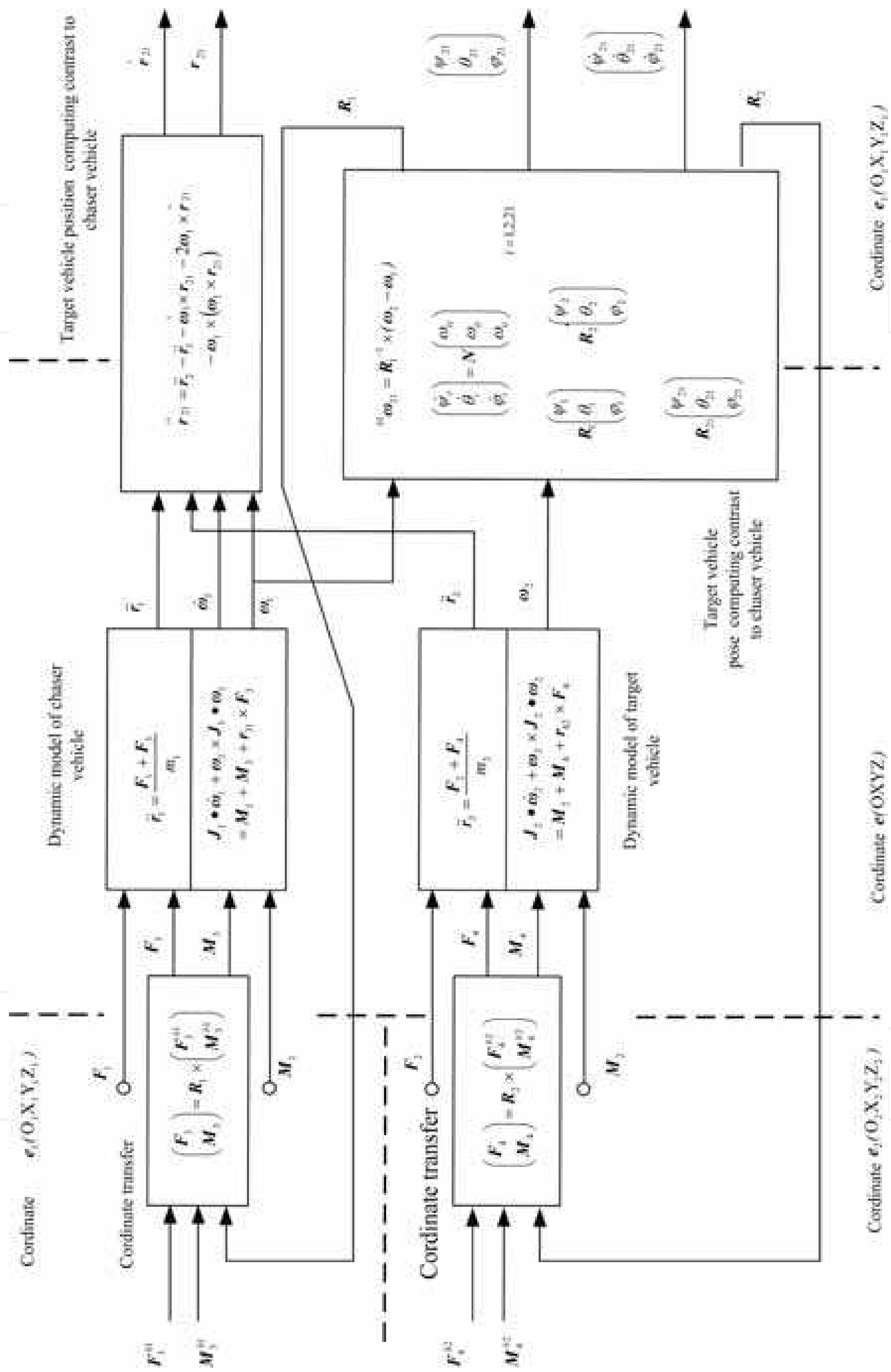

Fig. 5. Mathematic model of on-orbit docking spacecraft bodies

The displacement and force relationship of the docking mechanism in the X direction can be shown in Figure 6. The displacement and force relationship of the docking mechanism in the Y or in Z direction are nearly same, shown in Figure 7. The relationships between torque and yaw angle or pitch angle of the docking mechanism are nearly same, they are shown in Figure 8. The relationship between torque and roll angle of the docking mechanism are shown in Figure 9. Above figures indicates the complexity of the dynamics characteristics of docking mechanism.

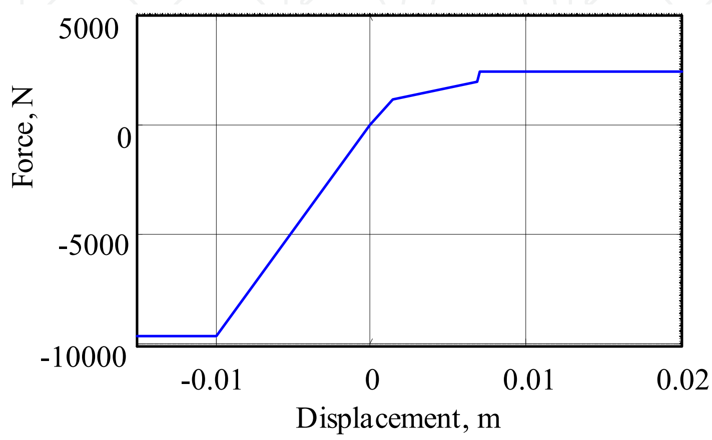

Fig. 6. Force and displacement in X direction

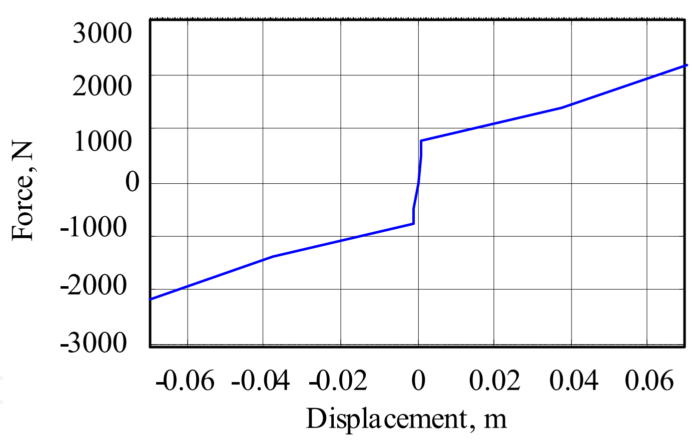

Fig. 7. Force and displacement Y or Z direction

The capturing and the impact absorbing are two main successive on-orbit docking phases for the on-ground HIL simulation (Peng et al., 1992). During the impact-absorbing phase, the docking mechanism shows strong coupling and nonlinearity and its parameters vary in large scale. During the capturing phase, the active docking mechanism on the chase vehicle collisions with the passive docking mechanism mounted on the target vehicle and the contact cases are very complicate (Guan, 2001). So it is difficult to describe the actual docking mechanism with the mathematical model, or it will abate the credence of the simulation. Thus, it is proper to use the physical model of docking mechanism, especially use full scale to docking/ berthing hardware as the physical model participating in the simulation.

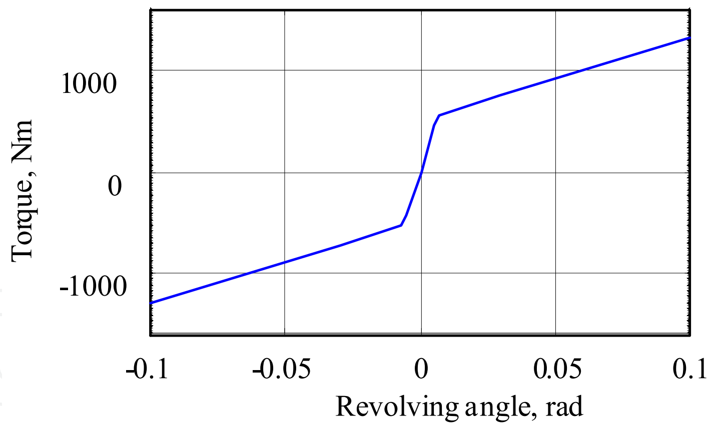

Fig. 8. Torque and angle in yaw and pitch

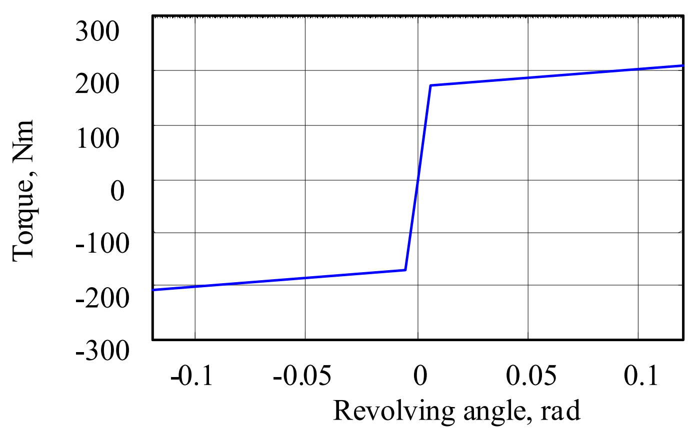

Fig. 9. Torque and angle in roll

3.5 Dynamics model of simulated system

If the mathematic model of the docking mechanism is established, its block diagram can connect with the block diagram of the docking dynamics model of spacecraft body. Then the dynamics model of simulated system is established, shown in Figure 11. Its reference frame is the body coordinate $\mathbf{e}_1(O_1X_1Y_1Z_1)$.

The mathematic model of the simulated system can be used to validate the correction of real-time simulation model of the HIL simulation system.

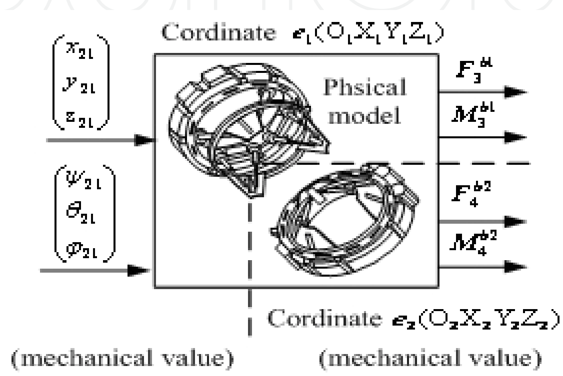

Fig. 10. Block diagram of docking mechanism

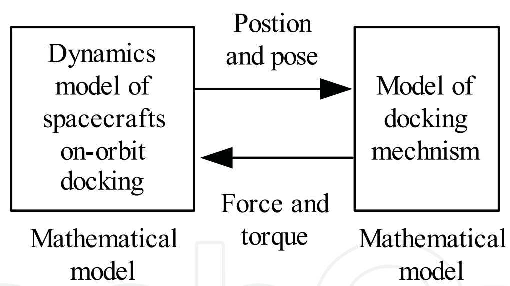

Fig. 11. Simulated system model

3.6 Frequency band width of docking dynamics

The rigidity in the longitudinal direction of the APAS 89 is bigger than that in other directions. The value of the rigidity is not a constant, it varies in large-scale. But it can be roughly divided as contacting rigidity and impact absorbing rigidity. The contacting rigidity is nearly 10^6 N/ m. Considering the mass of the spacecrafts, the frequency of the main dynamic process needed to be re-emerging by the HIL simulation is finite. The upper frequency bound is called as docking frequency, signed as ω_d and ω_d is usually no larger than 5 Hz. The dynamic process of spacecraft on-orbit docking is a high frequency response process, it requires that the motion simulator and the F/ T sensor should have high frequency response ability.

4. System construction ideas of HIL simulation for spacecraft on-orbit docking dynamics

The dynamics model of spacecraft on-orbit docking and the actual body of docking mechanism are two components of the HIL simulation. They come from the simulated system, shown in Figure 12. Before the constructing of HIL simulation system, the correction of the dynamic model of spacecrafts on-orbit docking should be verified.

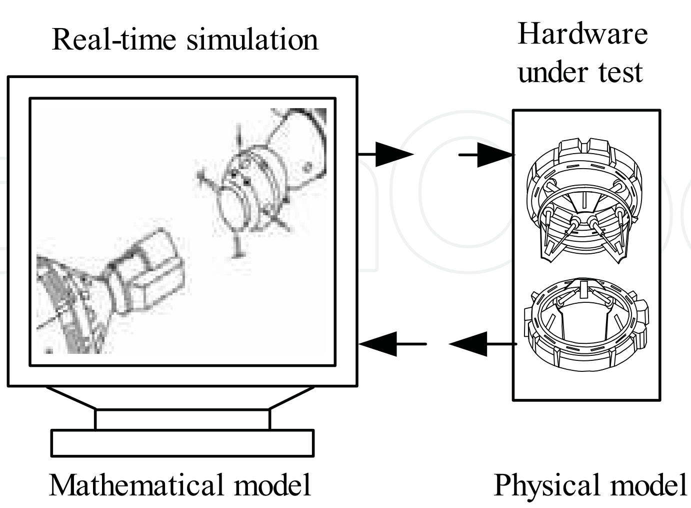

Fig. 12. Simulated system

The mathematic model of spacecraft on-orbit docking dynamics can run on real-time simulation computer, but it is not stand alone. The input signals of the real-time simulation

computer are the forces and torques values created by the docking mechanism, mean while the real-time simulation computer outputs the movement values of the spacecraft bodies.
Obviously, the actual docking mechanisms or their physical models can not be drive by the electrical signals created by the real-time simulation computer, and they can not provide the electrical signals of force and torque needed by the real-time computer either.
Here, a generalized interface concept is presented. The simulation/ hardware interface is a complex system, not an electrical interface. It connects the real-time simulation with the hard wares under test and sets up the HIL simulation system, shown in Figure 13. It may include electro-hydraulic system, electro-mechanical system, parallel manipulator, various sensors, and so on.
The simulation/ hardware interface of the HIL simulation system for spacecraft on-orbit docking dynamics consists of the motion simulator and the force and torque sensors. The motion simulator accepts the motion command signals created by the real-time simulation computer and outputs mechanical movements which can drive the docking mechanism. Then, the active dock mechanism and passive docking mechanism can collide with each other and produce force and torque. The force and torque sensor which is mounted on the rack picks up the force and torque acted by the active docking mechanism. This force and torque sensor can be imaged having been mounted between the passive docking mechanism and the target vehicle body. The force and torque sensor which is mounted on the moving plate of the Stewart platform picks up the force and torque acted by the passive docking mechanism. This force and torque sensor can be imaged having been mounted between the active docking mechanism and the chaser vehicle body. The actual forces and torques are transformed into the digital signals which can be collected by the real-time simulation computer. Now, the main feedback loop of the HIL simulation system is established. It is called two force and torque sensor scheme.

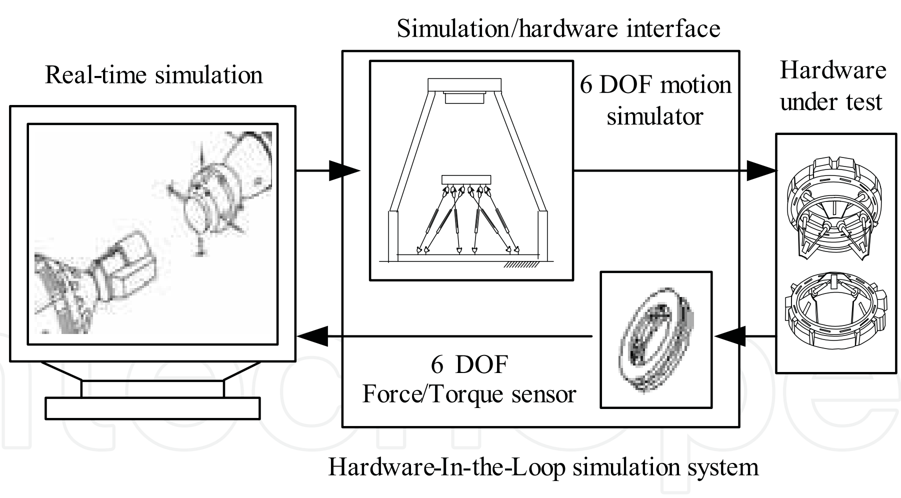

Fig. 13. HIL simulation system

The dynamic characteristics of the feedback system of the HIL simulation system are required to be similar with those of the simulated system. But unfortunately the dynamic characteristics of the simulation/ hardware interface distort the similarity, especially for the high frequency response dynamics simulation. If the dynamic characteristics of the feedback system are not properly rebuilt, the dynamic characteristics of the HIL simulation system are quietly different with those of simulated system. For an example, the simulated system is always stable, but its HIL simulation may be unstable. This is the fundamental reason of the system design problem or system integrated problem. So the system design problems or

system integrated problems (Chang et al., 2007a) are put forward. But the system construction of the HIL simulation for the spacecraft on-orbit docking dynamics is difficult.
The main part of the motion simulator of the simulation/ hardware interface is a Stewart platform driven by six electro-hydraulic servo systems, it is a nonlinear and strong coupling multi-input multi-output (MIMO) system. The dynamic model of spacecrafts on-orbit docking is also a nonlinear and strong coupling MIMO system. Further more, the actual docking mechanism is included into the HIL simulation, the docking mechanism is a very complex electro-mechanical system. It may be controlled or operated by a human. So the HIL simulation system is too complex to study as a whole system. That is why the ideas of simulation/ hardware interface of HIL simulation system for spacecraft on-orbit docking is put forward.
The system design procedure based on the concept of the simulation/ hardware interface is illustrated in Figure 14. It is expected to find the criterion or guideline to the design of the simulation/ hardware interface, through analyzing the HIL simulation system. The guide line of the simulation/ hardware interface design can be gained through analyzing the guide line of the HIL simulation. During system design period, design problem of the complex HIL simulation system is simplified as a comparatively simple design problem of simulation/ hardware interface.

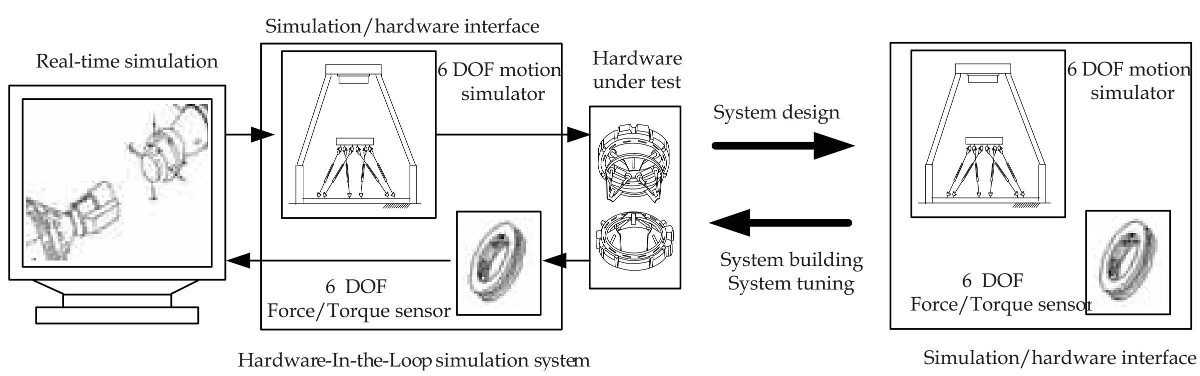

Fig. 14. HIL simulation system design, system building and system tuning

During system tuning or system building period, the object of the system tuning is simulation/ hardware interface. Through tuning the dynamic characteristics of the simulation/ hardware interface, the dynamic characteristics of the whole HIL simulation system can be adjusted to meet the requirements of simulation.
If un-modelled dynamic characteristics are omitted, the real-time simulation and the hardware under test do little to the authenticity of the HIL simulation based on above system construction ideas, because they are the components of the simulated system. In another word, above system construction ideas ensure the adaptability of the HIL simulation system to the docking mechanism and to the spacecraft.
And this is the fundamental base that a simplified docking mechanism can be used to validate the HIL simulation system. This is another merit of above HIL simulation system construction ideas.
The initial capture condition and locus planning model block is added into above HIL simulation, the basic system structure of HIL simulation for on-orbit docking is shown in Figure 15. The locus planning programme drives the motion simulator to make the passive docking mechanism to collide with active docking mechanism mounted on the rack with the initial test conditions. And just before capturing, the feed back loop of the dynamics control is closed.

5. Research procedure to technology of HIL simulation for spacecraft on-orbit docking dynamics

Because of the complexity of the HIL simulation system construction for spacecraft on-orbit docking dynamics, the analysis and synthesis of the HIL simulation system for on-orbit docking is still difficult today yet, because there are many obstacles involving in them. The main obstacles that are brought into the HIL simulation system design by the hardware under test are strong nonlinearity and strong coupling of the docking mechanism, the high equivalent rigidity of the docking mechanism and the large-scale varying of the rigidity. The high-speed response dynamic process of on-orbit docking and the high accuracy of the simulation requirement make the HIL simulation design even more difficult. Furthermore, the nonlinear and the coupling of mathematic model of the spacecraft on-orbit dynamics, the nonlinear and the coupling of motion simulator further hinder people to analyze or to synthesize the HIL simulation system with theoretical method.

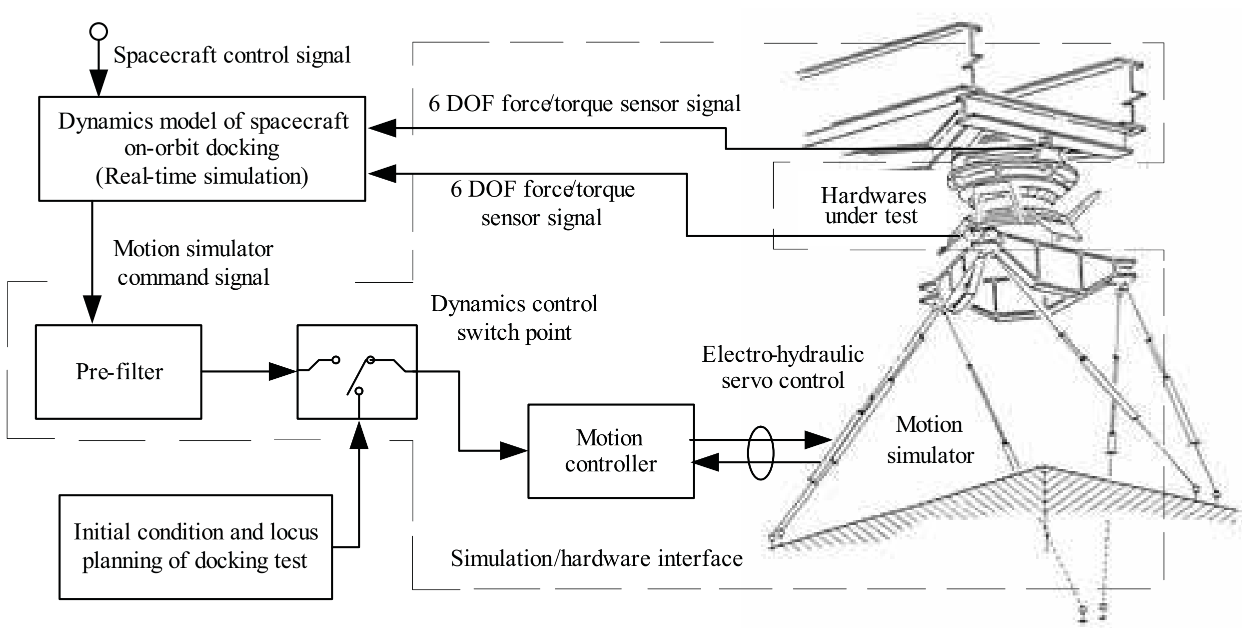

Fig. 15. Basic system structure of HIL simulation for on-orbit docking

Obviously, it is an easy to research the design guideline of the HIL simulation system with single degree-of-freedom (DOF) model, which is the simplified model of the actual spacecraft on-orbit docking.
So the first step of the research procedural is to research design guideline of the HIL simulation system with the single DOF model, then the results of the single DOF model can be extended to the MIMO HIL simulation system case through theoretical analysis and experimental validation.

6. System construction procedure to HIL simulation for single-degree-of-freedom spacecraft on-orbit docking dynamics

The single DOF HIL simulation system is a single-input single-output (SISO) system. Since ultimate aim of the SISO system research is helping find the design guideline of MIMO system. Even though it is not difficult to analyze or synthesize the single HIL simulation system as the whole system, the research on single DOF model will strictly follow the ideas of simulation/ hardware interface.

6.1 Single DOF HIL simulation system model

The actual spacecrafts on-orbit docking are simplified as a single DOF spacecraft on-obit docking, which is two single DOF spacecrafts docking with a simplified docking mechanism model. Under the idea of simulation/ hardware interface, the single DOF spacecrafts docking with a simplified docking mechanism model is segmented into two parts shown in Figure 16.

Then the model of HIL simulation system of a single DOF spacecraft on-orbit docking dynamics is set forth, it is illustrated with Figure 17. The force sensor and an electro-hydraulic servo-system driving actuator make up the simulation/ hardware interface.

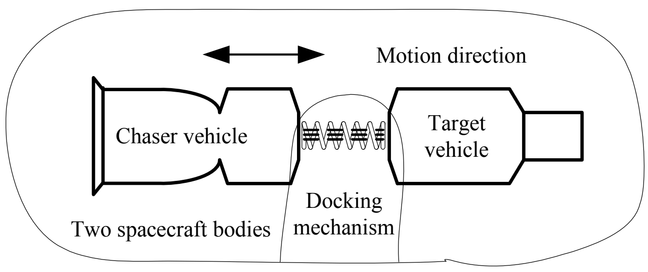

Fig. 16. Single DOF simulated system

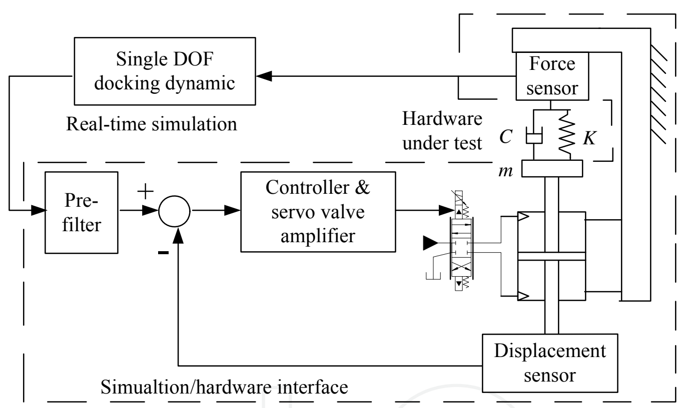

Fig. 17. Single DOF HIL simulation system

The single DOF spacecraft bodies are shown in Figure 18. x is defined as the relative displacement between the two spacecrafts, then

$$x = x_2 - x_1 \, . \tag{3}$$

The mathematic model for the real-time numerical simulation of the HIL simulation is the dynamics model of the two rigid bodies driven by a pair of acting and counteracting forces in the conditions of zero gravity and vacuum. By simple deriving, the dynamics model can be written as

$$G_{DDyn}(s) = \frac{X(s)}{F(s)} = \frac{m_1 + m_2}{m_1 m_2} \times \frac{1}{s^2} \, . \tag{4}$$

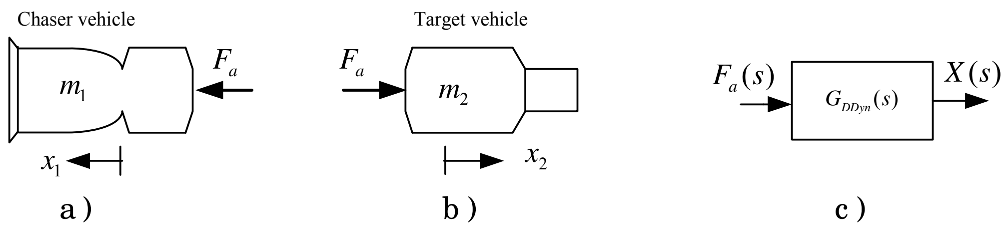

Fig. 18. Single-DOF spacecraft bodies

Above dynamics model is also a simplified version of the dynamics model actual spacecraft bodies shown in Figure 5.

The docking mechanism of the single DOF can be simplified as a spring and a damper, shown in Figure 19. Its mathematic model of the docking mechanism can be written as

$$G_{DMech}(s) = \frac{F(s)}{X(s)} = -Cs - K \quad (5)$$

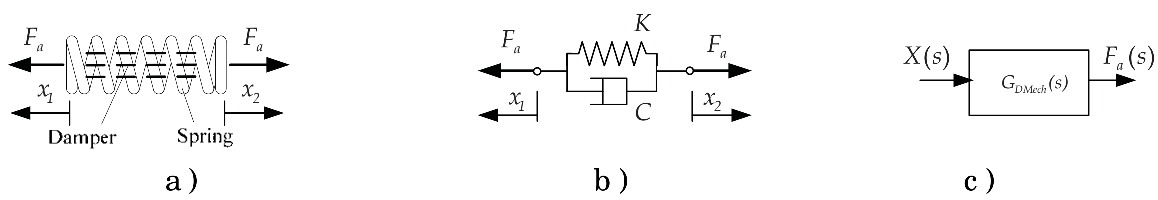

Fig. 19. Single-DOF docking mechanism

6.2 Ideas on simulation/hareware interface and control strategy on HIL simulation

When the docking mechanism is simplified as a spring-damp device, the single DOF simulated object system can be used to research the dynamic process of the face-to-face collision and impact absorbing process during spacecraft docking.

The dynamics characteristics of the simulated object system can be described by a feedback system shown in Figure 20, even though the mechanical structure of the simulated object system is open chain structure. The feedback characteristics are intrinsic and not obvious. Then

$$\frac{X_{mech}(s)}{F_r(s)} = \frac{G_{DDyn}(s)G_{DMech}(s)}{1 + G_{DDyn}(s)G_{DMech}(s)} \quad (6)$$

The HIL simulation system for on-orbit docking can be shown in Figure 21. The force sensor and the motion simulator are called as simulation/ hardware interface. It is the simplified version of the system shown in Figure 13.

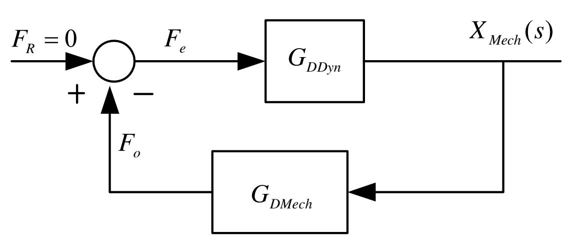

Fig. 20. Block diagram of simulated system

$$\frac{X_{mech}(s)}{F_r(s)} = \frac{G_{DDyn}(s)G_{DMech}(s)G_{FSensor}(s)G_{MSim}(s)}{1+G_{DDyn}(s)G_{DMech}(s)G_{FSensor}(s)G_{MSim}(s)} \quad (7)$$

Comparing Equation (6) and Equation (7), The dynamic characteristics of the HIL simulation system and those of the simulated system are the same when $G_{FSensor}(s)G_{MSim}(s)=1$.

Based on the idea of the simulation/ hardware interface, the function of the simulation/ hardware interface is to establish the connection between the physical model and the real-time simulation. The design guideline of HIL simulation system should be

$$G_I(s) = G_{FSensor}(s)G_{MSim}(s) \approx 1 \quad (8)$$

Where $s = j\omega$, for $0 \le \omega \le \omega_s$. ω_s is called as HIL simulation frequency in this paper.

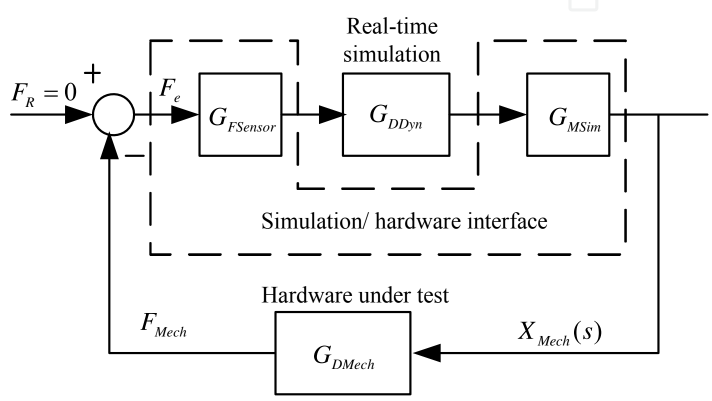

Fig. 21. Block diagram of HIL simulation system

To adapt to the characteristics of the docking mechanism, the HIL simulation frequency band is needed to cover the docking frequency band. That is $\omega_s \ge \omega_d$.

Above are the desired performances of the simulation/ hardware interface. Its realization is a control problem. Many control strategies can meet above demand. These solutions scheme can be summarized up as two-degree-of-freedom control structure, shown in Figure 22.

$$G_{MSim}(s) = Y_M(s)/X_M(s) = G_{prefilter}G_{Controller}G_{Actutor} \,/\, (1+G_{Controller}G_{Actutor}). \quad (9)$$

In two-degree-of-freedom control structure, $G_{Controller}$ is controller of feedback system, which help to reduce the variation of the plant output, while $G_{prefilter}$ is used as a filter to tailor the response of the simulation/ hardware interface to meet the specification of the HIL simulation system. The precondition of the compensation with $G_{prefilter}$ is that the sensitivity of the dynamic characteristics of the electro-hydraulic system to the variation of factors such as payload rigidity is lower in the docking frequency. In another word, the sensitivity of the pole positions in S domain of the close-loop transfer function of the motion simulator to the large-scale variation of payload stiffness is lower.

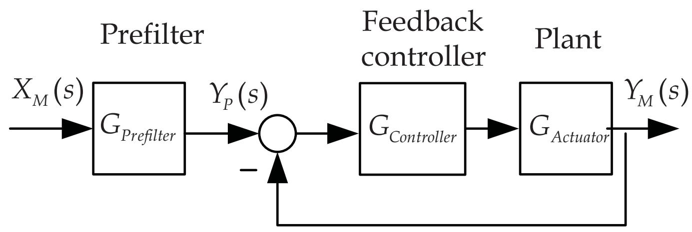

Fig. 22. Two-degree-of-freedom control structure

Once the control structure is made certain, the other control problems are the skills or methods to fulfill it.

To ensure the stability and the performance of the HIL simulation system, the error between $G_I(s)$ and 1 must be sufficiently small in the docking frequency band. The relationship between the distortion of the HIL simulation and above errors can guide the HIL system tuning (Chang et al., 2007d).

6.3 The key problems of the simulation/hardware interface design

The attribute of the simulation/ hardware interface requires that the motion simulator of the HIL simulation system should be with high accuracy and high response. The electro-hydraulic actuator helps the motion simulator achieve high speed response and high rigidity. Zhang (2006) presents that the amplitude error of the electro-hydraulic system of motion simulator at the middle position is no larger than 2 dB and the lag is no larger than 70 degrees when the frequency of input signal is 10 Hz.

The hardware (docking mechanism) under test is the load of simulation/ hardware interface. The large-scale variation of the rigidity of docking mechanism requires that the simulation/ hardware interface should be insensitive to them. This is the precondition of the HIL simulation system synthesis using the two-degree-of-freedom control structure. The method to solve above problems is tried to increase hydraulic spring rate of the electro-hydraulic actuator to make the natural frequency of the hydraulic actuator approximate to the hydraulic undamped natural frequency.

Here we only make a brief explanation on it.

The displacement output of the hydraulic power element of the motion simulator can be expressed as:

$$Y = \frac{\frac{K_q}{A} X_v - \frac{K_{ce}}{A^2}\left(\frac{V_t}{4\beta_e K_{ce}} s + 1\right) F}{\frac{V_t m}{4\beta_e A^2} s^3 + \left(\frac{m K_{ce}}{A^2} + \frac{B_c V_t}{4\beta_e A^2}\right) s^2 + \left(\frac{K V_t}{4\beta_e A^2} + \frac{B_e K_{ce}}{A^2} + 1\right) s + \frac{K K_{ce}}{A^2}} . \quad (10)$$

The symbols used here is as same as those in Merrit's book (Merrit, 1967). From equation (10), it can be known dynamic characteristics of the electro-hydraulic system will change when the stiffness of the payload is varying.

The hydraulic actuators could be designed to make the hydraulic spring rate of the hydraulic actuators much greater than the equivalent rigidity of the docking mechanism. That is to satisfy the following inequality by enlarging the effective area A of the hydraulic cylinder.

$$K / K_h << 1 \quad (11)$$

Where $K_h = 4\beta_e A^2 / V_t$. Then, the positions of the loop transfer function poles of the hydraulic power element are less sensitive to the rigidity variation of the payload. The positions of the close-loop poles of the electro-hydraulic system of the motion simulator are less sensitive to the rigidity variation of the docking mechanism (Chang et al., 2007c).

If working substance (oil) in the hydraulic system is done vacuum pumping, the bulk module of the working substance will be enlarged, K/K_h will be even smaller and the dynamic performance of the motion simulator will be less sensitive to the rigidity variation of the docking mechanism.

The force sensor adopted for the HIL simulation system is piezocrystal, which has higher rigidity. It can still achieve high natural frequency when it is attached on the docking mechanism. And the natural frequency of force sensor is possible to be higher than 350 Hz.

6.4 Validation with simulation

The simulation research is aim at verifying the design ideas of the simulation/ hardware interface, design guideline of the HIL simulation system and the simulation/ hardware interface, as well as the methods and skills for the system tuning. Single DOF spacecraft on-orbit docking is the simulated object.

The mathematic model of the single HIL simulation system for on-orbit docking dynamics is established with Matlab/ Simulink. The parameters of the motion simulator are shown in Table 1.

Symbol	Nomenclature	Value
A	Effective area of actuator	0.06m2
V_t	Total compressed volume of actuator	0.36m3
m	Mass load of motion simulator	2500kg
β_e	Bulk module of oil	6.9×10^{8} Pa
B_c	Viscous damping coefficient of motion simulator	20N/ (m· s-1)
K_{ce}	Total flow-pressure coefficient	9×10^{-12} m3/ (s· Pa)

Table 1. Parameters for single DOF motion simulator

The control structure of the motion simulator is shown in Figure 22. By tuning the controller $G_{prefilter}$, the performance of the motion simulator can be described as: when the frequency of the input signal is 10Hz, the amplitude error is not larger than 2dB and the phase error is no larger than 70 degrees.

Then $G_{Controller}$ is defined to make the simulation/ hardware interface transfer function $G_I(s)\approx 1$ when $0\le\omega\le\omega_s$, the Bode diagram of the simulation/ hardware interface is shown in Figure 23.

The Table 2 shows the parameters of the on-orbit docking spacecrafts. If the linear model of the docking mechanism is adopted by the simulated object system, and its parameters are shown in Table3, the dynamic characteristics of the HIL simulation system are described by curve a in the Bode diagram, shown in Figure 24. The dynamic characteristics of the simulated object system are described by curve b. The curve a and curve b superpose with each other at lower frequency.

Symbol	Nomenclature	Value
m_1	Mass of chaser vehicle	8000kg
m_2	Mass of target vehicle	12000kg

Table 2. Parameters of single DOF spacecrafts

The simulated object adopted the nonlinear docking mechanism model, its characteristics are shown in Figure 6, and the results of simulation are shown in Figure 25 and Figure 26. The damp model of the docking mechanism is simplified as the viscous damp and its value is 4000Ns/ m. In each figure, the curve a is the simulation result to the HIL simulation system; the curve b is the ideal result of the simulated object system model shown in Figure 16 but with the nonlinear docking mechanism model.

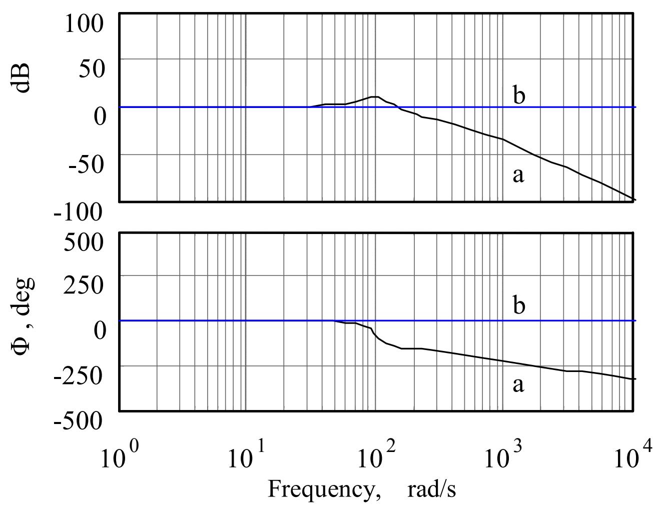

Fig. 23. Bode diagram of simulation/ hardware interface

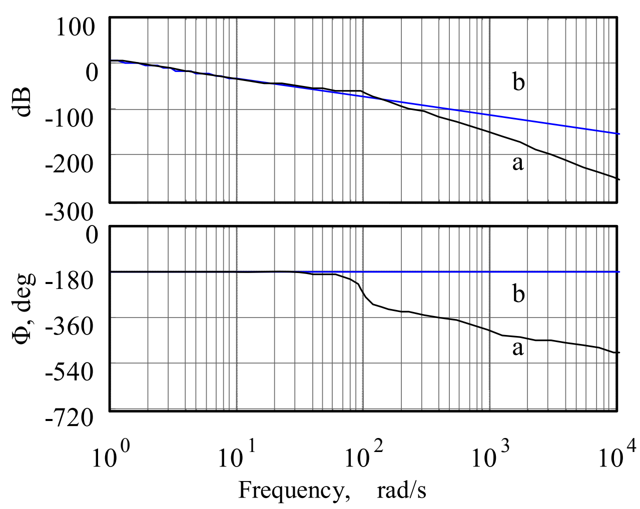

Fig. 24. Bode diagram of HIL simulation system

Symbol	Nomenclature	Value
K	Rigidity of docking mechanism	1000000N/ m
C	Viscous damping coefficient of docking mechanism	0 N/ (m· s-1)

Table 3. Parameters for single DOF linear docking mechanism

7. System construction procedure to HIL simulation for multi-degree-of-freedom spacecraft on-orbit docking dynamics

7.1 Actual HIL simulation system for spacecraft on-orbit docking dynamics

Since the simulated system is segmented in two parts, and they all take part into the HIL simulation system in different forms. The actual docking mechanisms are the hardwares under test. The mathematic model of the real-time simulation is established with the spacecraft bodies, it can be described by Figure 27.

Based on the experience of the system construction of the single DOF spacecraft docking dynamics, the piezoelectricity 6-DOF force and torque sensors are adopted as the interface from the hardware to the real-time simulation. To drive the passive docking mechanism, a Stewart platform and a fixed rack are used as the motion simulator, it is the interface from real-time simulation to hardware. The six legs of the Stewart platform are driven by six electro-hydraulic servo control system. The response speed and rigidity of the motion simulator are all high.

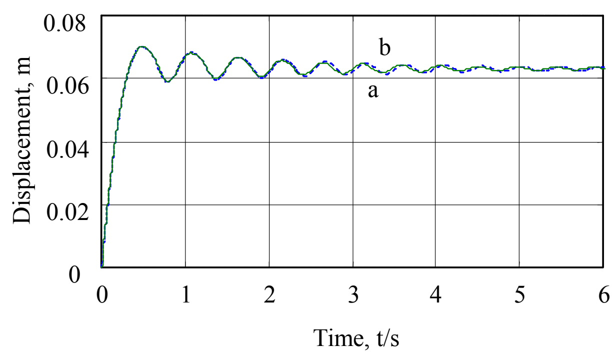

Fig. 25. Displacement curves

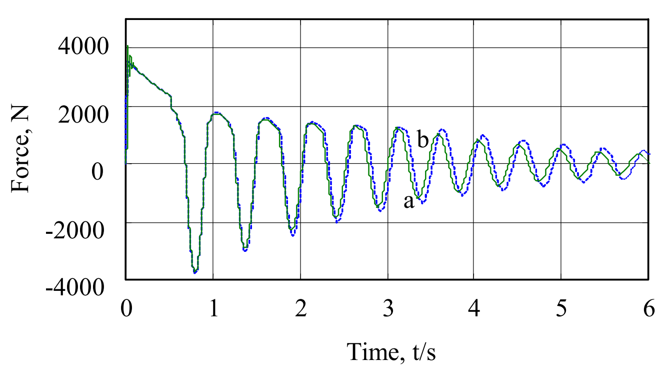

Fig. 26. Force curves

The reference frame $\boldsymbol{e}_b(O_bX_bY_bZ_b)$ is set on the ground. $\boldsymbol{e}_0(O_0X_0Y_0Z_0)$ is set on the fixed rack, and $\boldsymbol{e}_p(O_pX_pY_pZ_p)$ is set on the moving plate of the Stewart platform. Their directions are shown in Figure 27.

Figure 28. shows the relationship between the reference frame of the motion simulator and the reference frame of spacecrafts bodies. It shows the transform from the position and pose signal of the spacecraft bodies of real-time simulation model to the command signal of the motion simulator.

In engineering, the two force and torque sensor scheme of the HIL simulation system bring some difficult in system tuning. When the mass of moving part of the active docking mechanism is relatively small, the force and torque sensor can be calculated out with signals from the force and torque sensor fixed on the rack by Equation (12) and Equation (13). The force and torque sensor mounted on the moving plate of the motion simulator can be omitted. And this is called single force and torque sensor scheme.

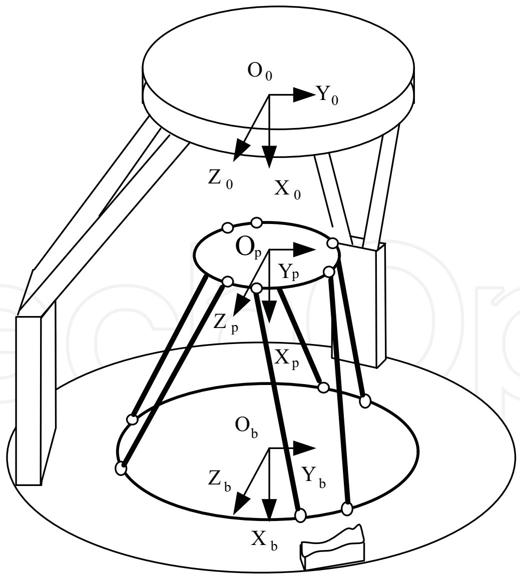

Fig. 27. Reference frame of motion simulator

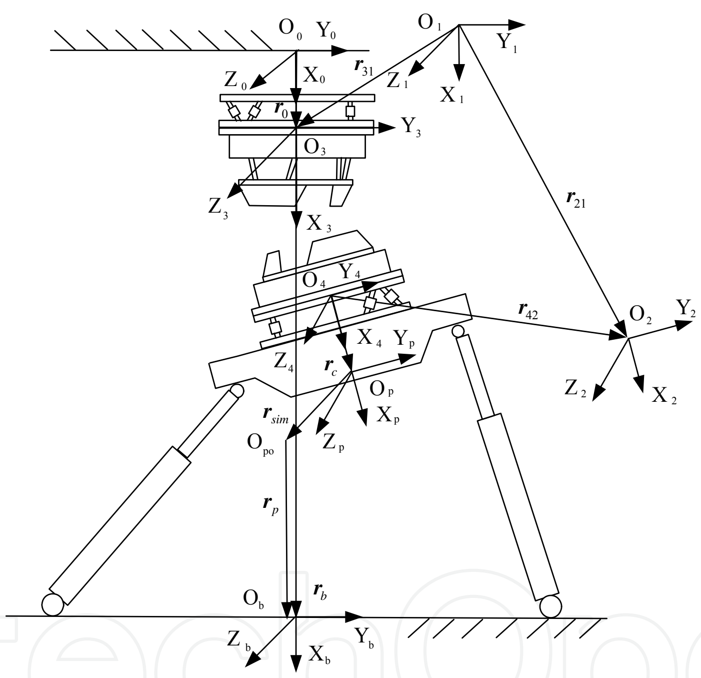

Fig. 28. Reference frame of HIL simulation

$$\boldsymbol{F}_4 = -\boldsymbol{F}_3 = \boldsymbol{F}' = -\boldsymbol{F} \tag{12}$$

$$\boldsymbol{M}_4 = (\boldsymbol{r}_{21} + \boldsymbol{r}_{42} - \boldsymbol{r}_{31}) \times \boldsymbol{F}_4 - \boldsymbol{M}_3 \tag{13}$$

7.2 Design issues on simulation/hardware interface

The natural frequency can be used as an index to evaluate the dynamic performance of a mechanical system. The natural frequency of the force and torque sensor is much higher than that of the motion simulator. So the dynamic characteristics of the simulation/hardware interface are limited by the Stewart platform of motion simulator. The Stewart platform is a typical parallel manipulator, the design of the Stewart platform is relative complex. Because of the limitation of pages, the design of the Stewart platform isn't discussed in detail, and only some research conclusions are listed here. By the way, some literatures (Lim et al., 1989; Merlet, 2000; He, 2007) can provide more detail information on this topic.

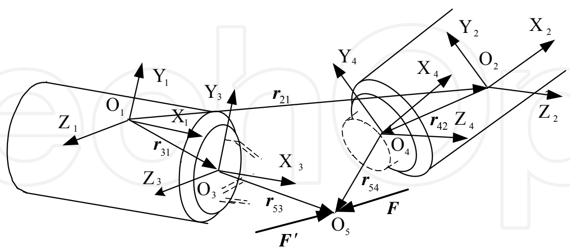

Fig. 29. Action and counteraction between spacecrafts

From former research results, it is reasonable to expect that the MIMO simulation/ hardware interface is decoupled and its dynamic performance is robust. Unfortunately, the research on the Stewart platform shows that it can not full decoupled, the dynamic characteristics of each degree of freedom of the Stewart platform will change when its position and pose is changing. How ever the variation of the dynamic characteristics of each degree of freedom of the Stewart can be reduced through its structure design.

Some research conclusions about the simulation/ hardware interface design are listed here.

- Large-dimension Stewart platform is adopted to improve the decoupling and robust ability of dynamic performance of the Stewart platform. The docking work space is much smaller than the reachable work space of the Stewart platform.
- Stewart platform is driven by electro-hydraulic servo control systems to gain high-peed performance and high-rigidity.
- Single rode symmetry electro hydraulic cylinder is used to enhance the robust ability of dynamic performance.
- The effective areas of the hydraulic actuator are enlarged to reduce the sensitivity of the electro-hydraulic system to the large-scale variation of the payload ridigity. (the same as the issues on single-DOF model)
- The working substance (oil) in the hydraulic system is done vacuum pumping to enhance the bulk module of the working substance will be enlarged and to further reduce the sensitive of dynamic performance of the motion simulator to the large-scale varation of rigidity of the docking mechanism.

Under above conditions, the coupling between the degrees of freedom can be treated as the un-modelled dynamic characteristics. Then the research results of single DOF HIL simulation can be used on each degree of freedom of the MIMO HIL simulation system for spacecraft on-orbit docking.

7.3 Analysis on motion simulator

The chief part of the motion simulator is a hydraulic driven Stewart platform. With the parameters of DDTS, the reachable space of the motion simulator is shown in Figure 30. Mean while the docking work space can also be drawn in same reference frame. Obviously the docking work space is the small space at the core of the reachable space of the Stewart platform. This feature of Stewart platform structure is help to reduce the variation of the dynamic characteristics of each degree of freedom of the Stewart platform in the docking work space.

By checking the natural frequency of the degree of freedom of the Stewart platform, the changing of its dynamic characteristics can be verified to meet the demands of the synthesis of HIL simulation system. In the upmost area of the docking work space, natural frequency of the degree of freedom of the Stewart platform is show in Figure 31, 32, 33, 34, 35 and 36.

7.4 Validation with experimental test

Base on the VV&A (Verification, Validation, and Accreditation) principles of system modeling and simulation, especially the priority objective principle and necessary but insufficient principle, the validation model used to check the authenticity of the HIL simulation results for spacecraft on-orbit docking dynamics is established. The validation model is a simplified spacecraft on-orbit docking model.

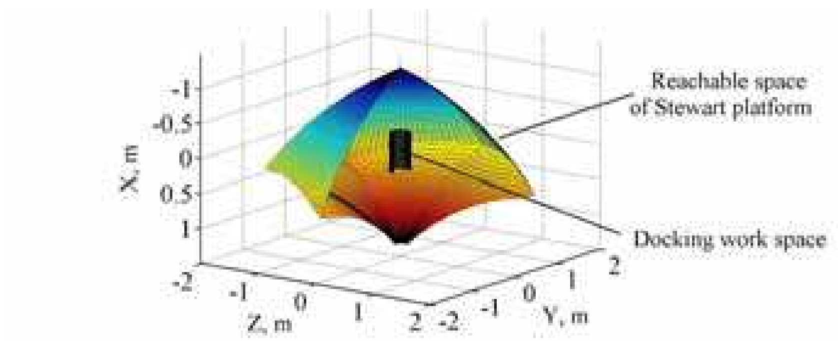

Fig. 30. Docking working space and reachable space of Stewart platform

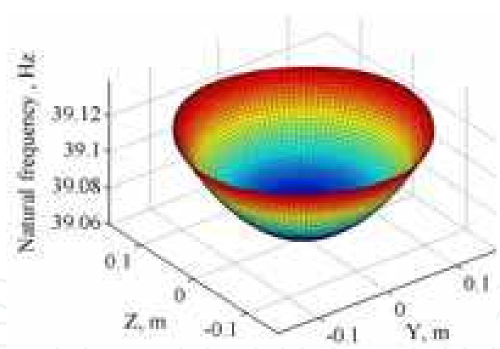

Fig. 31. Natural frequency in X direction

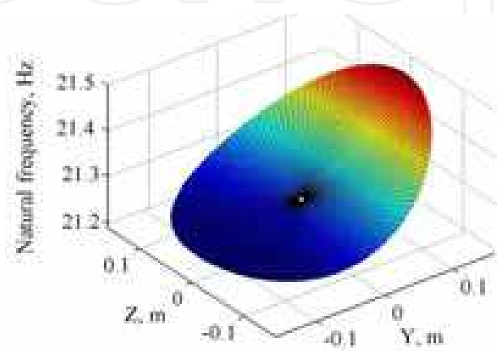

Fig. 32. Natural frequency in Y direction

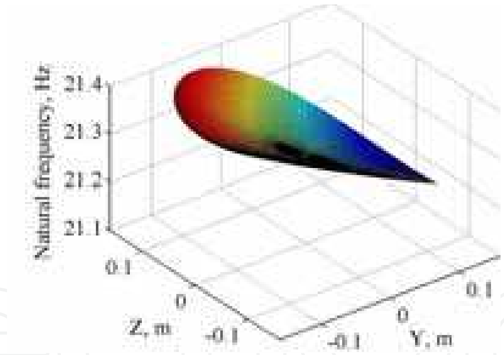

Fig. 33. Natural frequency in Z direction

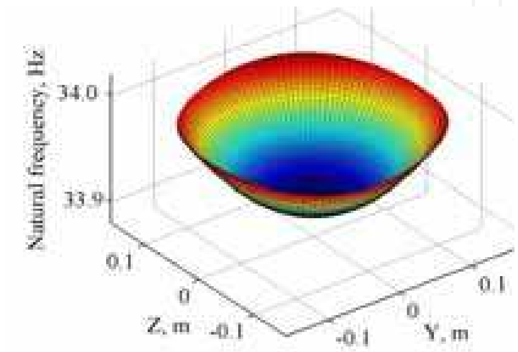

Fig. 34. Natural frequency in roll

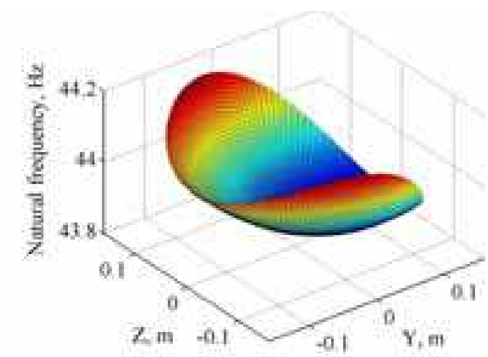

Fig. 35. Natural frequency in yaw

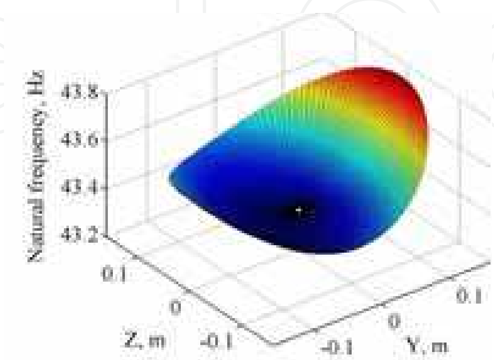

Fig. 36. Natural frequency in pitch

The validation model which can be simulated with the HIL simulation system is the simplified model of the simulated object system. The similarity between key parameters of the collision created by the hardwares of HIL simulation system and by the validation model can be used to check the dynamic characteristics of the closed-loop HIL simulation system.

Figure 37 shows the validation model of the HIL simulation system of on-orbit docking dynamics. The collision created by non-damping spring stick and a rigid frame is used to simulate the collision between the two spacecrafts. The spring stick is a cantilever, and its deformation is small. Since the collision is happened at the same point on the spring stick, the spring stick can be regarded as a spring and its spring rate K can be worked out by Equation (14).

$$K = 3\pi E d^4 / (64 l^3) \tag{14}$$

where E is the bulk module of material, N/ mm²; l is the nominal length of the spring stick; d is the diameter of the spring stick.

Omitting the damping of the spring stick caused by deformation (such as material damping, structural damping, etc.), the force relationship between elastic collision devices of the validation model is expressed in Equation (15).

$$F(x) = \begin{cases} -K(x - h/2 + d/2), & x > h/2 - d/2 \\ 0, & h/2 - d/2 \geq x \geq -h/2 + d/2 \\ -K(x + h/2 - d/2), & x < -h/2 + d/2 \end{cases} \tag{15}$$

where $F(x)$ stands for the collision force between the two spacecrafts, N; x stands for the relative displacement between the two spacecrafts, m; h see Figure 37, m.

The dynamics model of the mass bodies of the validation model is shown in Equation (16).

$$\ddot{x} = F(x) / [m_1 m_2 / (m_1 + m_2)] \tag{16}$$

where m_1 and m_2 are the mass of the mass bodies, kg.

Then the collision contact time of the validation model can be work out by Equation (17).

$$T_v = \pi \sqrt{m_1 m_2 / ((m_1 + m_2) K)} \tag{17}$$

While, T_h is the contact time of the collision created by the HIL simulation system. The similar ratio between the collision contact time R_T can be worked out by Equation (18).

$$R_T = T_h / T_v = T_h \sqrt{(m_1 + m_2) K / (m_1 m_2)} \Big/ \pi \tag{18}$$

If the damp of the validation model is omitted, the velocity recovery coefficient of the collision described by validation model e_v equals 1. The similarity ratio of the speed recovery coefficient R_e can be work out by Equation (19).

$$R_e = e_h / e_v = | v_1 | / | v_0 | \tag{19}$$

Where v_0 is the initial velocity, v_1 is bounce velocity, they can be read out from the velocity curve of the experimental results of the HIL simulation.

Obviously, if there is no distortion in the HIL simulation result, then R_e =1, R_T =1.

The experimental system of the HIL simulation system for spacecraft on-orbit docking dynamics is shown in Figure 38. The mathematical dynamics model run on the real time computer is the dynamics model of the actual spacecraft bodies which are docking on orbit, but its parameters should be set according to the specific freedom degree under test.
The validation mechanism, which is used as a testing device to check the performance of the HIL simulation system, can be installed into the HIL simulation system as the hardware under test instead of the docking mechanism.
The validation mechanism should be designed under direction of the HIL simulation system construction ideas and the validation model.
Figure 36 shows the HIL simulation system with the validation mechanism. All parts of the validation mechanism but the spring stick can be regard as the rigid bodies. The spring stick is used as a buffer device. Because the validation mechanism is the payload of the simulation/ hardware interface of the HIL simulation system, its mass, inertia, mass center should comfort to the actual docking mechanism.

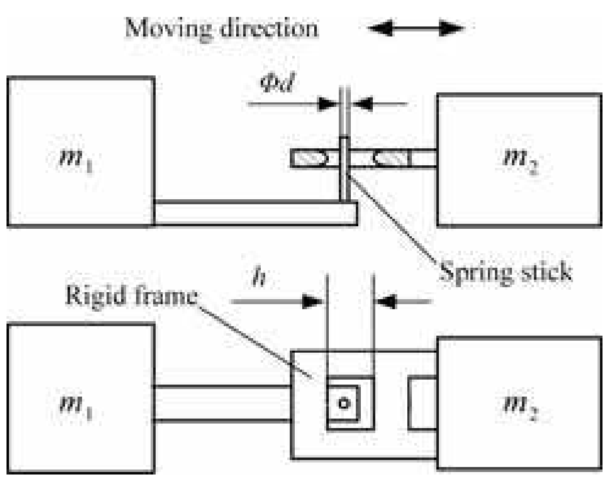

Fig. 37. Vibro-impact HIL simulation test

Fig. 38. Experimental validation system

Figure 39 and Figure 40 are Bode diagrams of motion simulator are tested in X direction and in Y direction respectively.

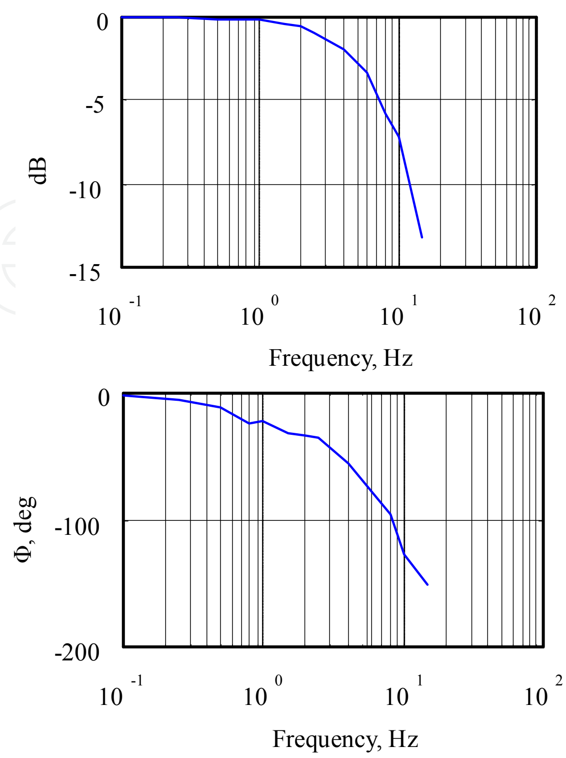

Fig. 39. Bode diagram in X direction

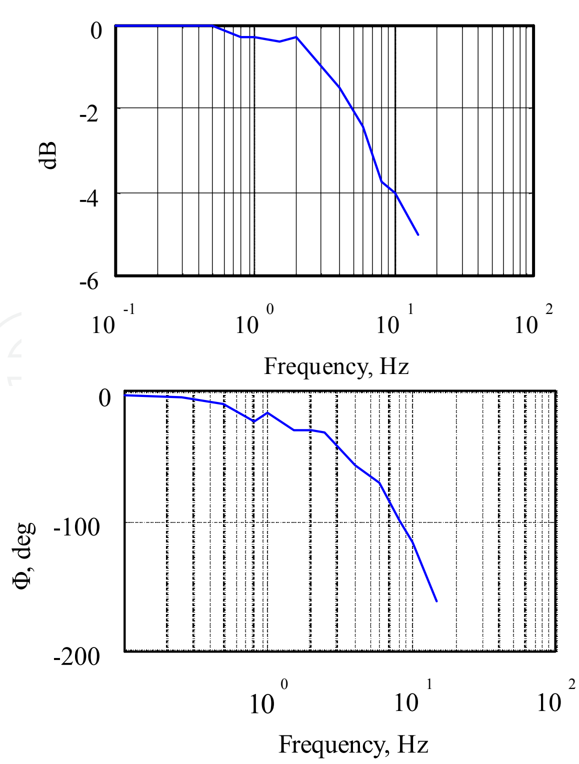

Fig. 40. Bode diagram in Y direction

If the dynamic characteristics of the HIL simulation system is not properly reconstructed with the time delay compensator, then if it is used to simulate the validation model (shown in Figure 37), the dynamic process of the HIL simulation system is divergent, shown in Figure 41 and Figure 42. By the way, above test is under control of the safe protection of the HIL system.
If the HIL simulation is over compensated, its dynamic process is not correct either, shown in Figure 43 and Figure 44.

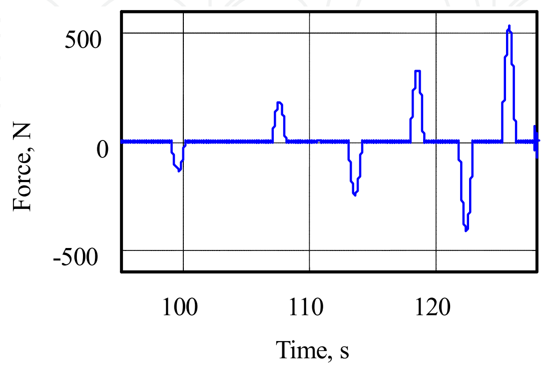

Fig. 41. Force curve

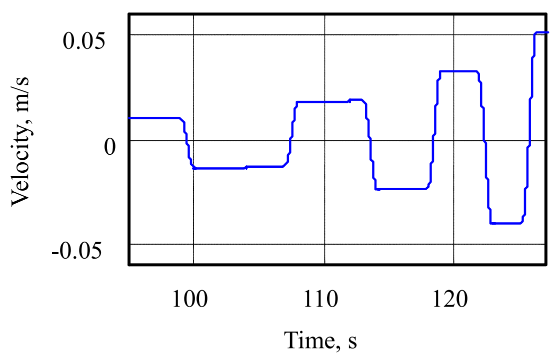

Fig. 42. Velocity curve

Test parameters			Test results			
			X direction		Y direction	
Frequency (Hz)	l (m)	$m_1 = m_2$ (kg)	R_e	R_T	R_e	R_T
0.235	0.140	32423	0.985	1.005	0.9725	1.019
0.471	0.140	8106	0.987	1.007	0.973	1.019
0.941	0.140	2026	0.95	0.988	0.96	1.016
1.731	0.100	1597	0.992	0.975	0.96	1.051
2.308	0.100	898	0.99	1.034	0.95	1.045
2.884	0.100	575	0.975	1.005	0.983	1.032

Table 4. Testing parameters & testing results

All above demonstrate that the HIL simulation system can not be used to simulate the spacecraft on-orbit docking dynamic process unless the dynamic characteristic of the HIL simulation system is properly reconstructed with the time delay and time lag of the compensator (Chang et al, 2007b).

After tuning the HIL simulation system, a set of tests are done in X direction and in Y direction respectively. The test parameters and the test results are shown in Table 4. Figure 45 and Figure 46 show the force curve and the velocity curve at 0.471Hz in X direction, while Figure 47 and Figure 48 show the force curve and the velocity curve at 0.471Hz in Y direction the test parameters. (Chang, 2010)

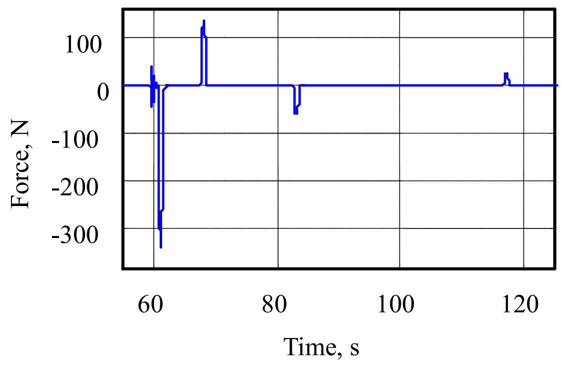

Fig. 43. Force curve

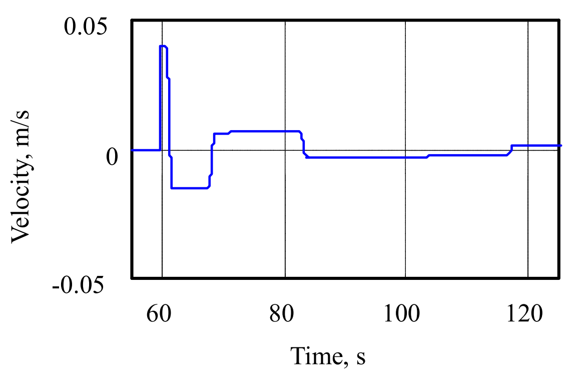

Fig. 44. Velocity curve

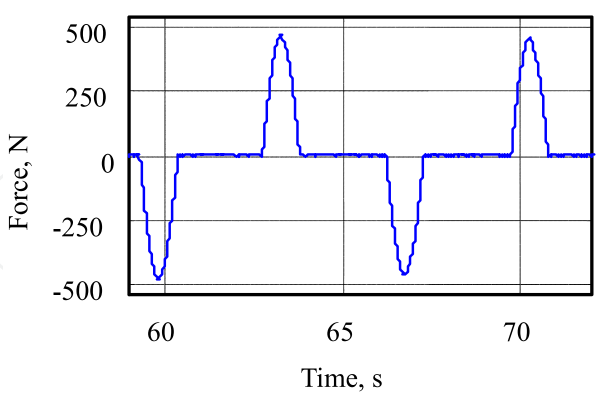

Fig. 45. Force curve

8. Conclusion

The ideas on the simulation/ hardware interface are presented. The simulation/ hardware interface is a complex mechtronics system, it connects the real-time simulation with the hard wares under test and sets up the HIL simulation system.

The ideas of the simulation/ hardware interface simplified the HIL system design and system building. The design problem of the complex HIL simulation system is simplified as a comparatively simple design problem of simulation/ hardware interface. Through tuning the dynamic characteristics of the simulation/ hardware interface, the dynamic characteristics of the whole HIL simulation system can be rebuilt.

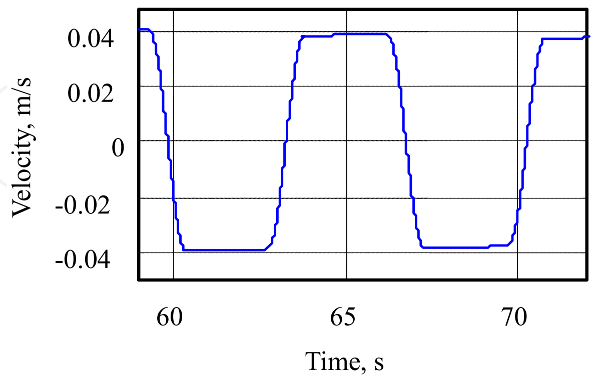

Fig. 46. Velocity curve

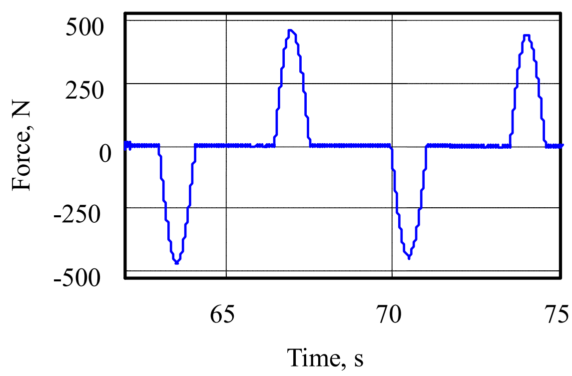

Fig. 47. Force curve

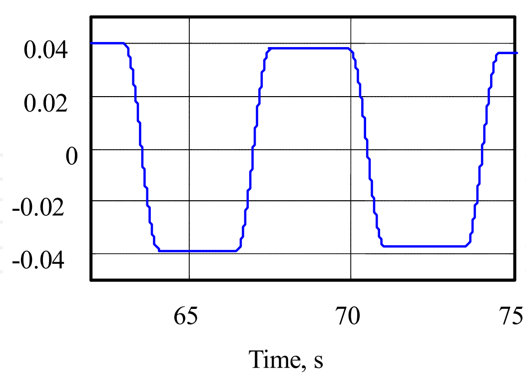

Fig. 48. Velocity curve

Based on the ideas on the simulation/ hardware interface, the design procedural of the HIL simulation can be divided into following steps: the segmentation of the simulated system, the establishing of the mathematic model, the design of the simulation/ hardware interface and the building of the whole system of HIL simulation.

The research on the single DOF HIL simulation system for spacecraft on-orbit docking dynamics verified the correction and feasibility of the ideas and procedural of the HIL simulation system construction. Then the research results of single DOF HIL simulation can be used on each degree of freedom of the MIMO HIL simulation system for spacecraft on-orbit docking. And its validation was done on an experimental system.

Further research work may be focused on the system building theory or system synthesis theory of multi-DOF HIL simulation for spacecraft on-orbit docking,. It is a promising research field.

9. References

Ananthakrishnan, S.; Teders, R. & Alder, K. (1996). Role of estimation in real-time contact dynamics enhancement of space station engineering facility. IEEE Robotics &Automation Magazine, Sep. 1996, pp.20-27

Chang, T. L.; Cong, D. C.; Ye, Z. M. & Han, J. W. (2007a). A new procedural for the integration of the HIL simulation system for on-orbit docking. Proceedings of the 2007 IEEE International Conference on Integration Technology, pp.769-773, ISBN Shenzhen Institute of Advanced Technology, Mar. 2007, IEEE, Shenzhen, China.

Chang, T. L.; Cong, D. C.; Ye, Z. M. & Han, J. W. (2007b). Time problems in HIL simulation for on-orbit docking and compensation. Proceedings of the 2nd IEEE Conference on Industrial Electronics and Applications (IEEE ICIEA 2007) , pp.841-846. IEEE Industrial Electronics (IE) Chapter & Harbin Institute of Technology, Ma. 2007, Harbin, China ,

Chang, T. L.; Cong, D. C.; Ye, Z. M. & Han, J. W. (2007c). Electro-hydraulic servo control system design of HIL simulator for spacecraft on-orbit docking. Proceedings of the Fifth International Symposium on Fluid Power Transmission and Control (ISFP2007), Yansan University, Beidaihe, China, Jul. 2007: 580~584.

Chang, T. L.; Cong, D. C.; Ye, Z. M. & Han, J. W. (2007d). Interface issues in Hardware-In-the-Loop simulation for spacecraft on-orbit docking. Proceedings of the Sixth IEEE International Conference on Control and Automation (IEEE ICCA 2007) , IEEE Control Systems Chapter (Singapore) & IEEE Control Systems Chapter (Guangzhou), Guangzhou, China, Jun. 2007: 2584-2590.

Chang, T. L.; Cong, D. C.; Ye, Z. M. & Han, J. W. (2007e). Simulation on HIL ground experimental simulator for on-orbit docking dynamics. Acta Aewnautica et Astwanautica. Vol.28, No.4, Jul. 2007, pp.975-980(in Chinese)

Chang, T. L.; Cong, D. C.; Ye, Z. M. & Han, J. W. (2008). Research on fundamental problems and the solutions of HIL simulation for on-orbit docking dynamics. Journal of Astronautics. Vol.29, No.1, Jan. 2008, pp.53-55(in Chinese)

Chang, T. L. (2010). Research on verification of authenticity of HIL simulation using vibro-impact model. Journal of Vibration and Shock. Vol.29, No.1, Jan. 2010, pp.22-25 (in Chinese)

Gates, R. M. & Graves, D. L. (1974). Mathematical model for the simulation of dynamic docking test system (DDTS) active table motion. N74-33776, pp.1-3

Grimbert, D. & Marchal, P. (1987). Dynamic testing of a docking system. N88-19516, pp.281-288

Guan, Y. Z.(2001). Research on dynamics and simulation technique of spacecraft docking process. Ph. D. thesis. Harbin, China: Harbin Institute of Technology, Aug. 2001, pp.8-12 (in Chinese)

He, J. F.(2007). Analysis and control of hydraulically driven 6-DOF parallel manipulator. Ph. D. thesis. Harbin, China: Harbin Institute of Technology, Feb. 2007, pp.89-98 (in Chinese)

Huang, Q. T.; Jiang, H. Z.; Zhang, S. Y. & Han, J. W. (2005). Spacecraft docking simulation using HIL simulator with Stewart platform. Journal of Chinese Mechanical Engineering. Vol.18, No.3, Mar. 2005, pp.415-418

Kang, J.; Guan, H. H. & Song, J.(1999). Study on dynamics of mechano-electronic spring-damper system with differential connections. J. Tsinghua Univ. (Sci. & Tech.) Vol.39, No.8, Aug. 1999, pp.68-71

Kawabe, H.; Inohira, E.; Kubota, T.; Uchiyama, M. (2001). Analytical and experimental evaluation of impact dynamics on a high-speed zero G motion simulator. Proceedings of the 2001 IEEE/ RSJ International Conference on Intelligent Robots and Systems. Hawaii, USA, Oct. 2005, pp.39~45.

Lange, C.; Martin, E.; Piedboeuf, J. C.; Kovecses, J. (2002). Towards Docking Emulation Using Hardware in the Loop Simulation with Parallel Platform. Proceedings of the Workshop on Fundamental Issues and Future Directions for Parallel Mechanisms and Manipulators. Quebec, Canada, Oct. 2002, pp.1-4

Lim, G. K.; Freeman, R. A.; Tesar, D. (1989). Modelling and Simulation of a Stewart Platform Type Parallel Structure Robot. The University of Texas at Austin, 1989, pp.1-151

Merlet, J. P. (2000). Parallel robots. Dordrecht: Kluwer Academic Publishers, 2000.

Merrit, H.E. (1967). Hydraulic control systems. New York: Wiley, 1967

Monti, A.; Figueroa, H.; Lentijo, S.; Wu, X. & Dougal, R. (2005). Interface issues in Hardware-in-the-Loop simulation. Proceedings of the 2005 IEEE Ship Technologies Symposium, Jul. 2005, pp.39-45

Office of Naval Research's Best Manufacturing Practices. (1999). Report of survey conducted at NASA Marshall Space Flight Center. Best Manufacturing Practice Center of Excellence. Huntsville, USA, Apr. 1999, pp.12-13

Peng, C. R.; Qu, G. J.; Ma, Z. C. & Yu, J. Y. (1992). Russia large spacecraft dynamics and its testing technology. Spacecraft Engineering, No.3, Mar.1992, pp.1-7 (in Chinese)

Tian, H.; Zhao, Y. & Zhang, D. W. (2007). Movement simulator modelling and simulation in integrate test platform for docking mechanism. Journal of Astronautics. Vol.28, No.4, July 2007, pp.996-1001(in Chinese)

Wu, L. B.; Wang, X. Y. & Li, Q. (2008). Fuzzy-immune PID control of a 6-DOF parallel platform for docking simulation. Journal of Zhejiang University (Engineering Science). Vol.42, No.3, Mar.2008, pp.387-391(in Chinese)

Yan, H.; Ye, Z. M.; Cong, D. C.; Han, J. W. & Li, H. R. (2007). Space docking hybrid simulation prototype experiment system. Chinese Journal of Mechanical Engineering. Vol.43, No.9, Sep.2007, pp.51-56(in Chinese)

Yu, W.; Yang, L. & Qu, G. J. (2004). Dynamics analysis and simulation of spacecraft docking mechanism. Journal of Dynamic and Control, Vol.2, No.2, Feb.2004, pp. 38-42 (in Chinese)

Zhang, C. F. (1999). Study on Six-Degree-of-Freedom simulation for docking. Aerospace Control, No.1, Jan. 1999, pp.70-74 (in Chinese)

Zhang, S. Y. (2006). Research on force control of hydraulic driven 6-DOF parallel robot. Ph. D. thesis. Harbin, China: Harbin Institute of Technology, Apr. 2006, pp.6-7 (in Chinese)

Zhao, H. & Zhang, S. Y. (2008). Stability analysis of the whole dynamics simulation system of space docking. J. of Wuhan Uni. of Sci. & Tech. (Natural Science Edition) Vol.31, No.1, Feb.2008, pp.87-97(in Chinese)

Zhao, Y; Tian, H. & Wang, Q. S. (2007). Analysis of dynamometry scheme for semi-physical simulation platform of space docking mechanism. Advances in Engineering Software. Vol.38, 2007, pp.710-716

Advances in Spacecraft Technologies
Edited by Dr Jason Hall

ISBN 978-953-307-551-8
Hard cover, 596 pages
Publisher InTech
Published online 14, February, 2011
Published in print edition February, 2011

The development and launch of the first artificial satellite Sputnik more than five decades ago propelled both the scientific and engineering communities to new heights as they worked together to develop novel solutions to the challenges of spacecraft system design. This symbiotic relationship has brought significant technological advances that have enabled the design of systems that can withstand the rigors of space while providing valuable space-based services. With its 26 chapters divided into three sections, this book brings together critical contributions from renowned international researchers to provide an outstanding survey of recent advances in spacecraft technologies. The first section includes nine chapters that focus on innovative hardware technologies while the next section is comprised of seven chapters that center on cutting-edge state estimation techniques. The final section contains eleven chapters that present a series of novel control methods for spacecraft orbit and attitude control.